Original Research

Revista Brasileira de Física Médica (2026) 20:884

Spatial Resolution Analysis via MTF: A Comparative Study of ImageJ (COQ Plugin), IAEA ATIA, and the Coltman Method

Jonas Nanni Menino[1], Tulio Guilherme Soares Marques[1,2], Raissa Alexia Camargo Guassu[1,2], Daniel Molena Seraphim[1,2], Diana Rodrigues de Pina[3]

[1]*Institute of Biosciences of Botucatu (IBB-UNESP), Botucatu, Brazil*
[2]*Clinical Hospital of the Botucatu Medical School (HCFMB-UNESP), Botucatu, Brazil*
[3]*Department of Infectious Diseases, Dermatology, Diagnostic Imaging, and Radiotherapy, Botucatu Medical School, Botucatu, Brazil*

Abstract

Spatial resolution, although commonly assessed qualitatively, can be quantified by determining the system's Modulation Transfer Function (MTF). The literature is extensive regarding methods for determining MTF in digital radiology equipment. Among the methodologies are semi-automatic methods, which require image analysis with dedicated software, and manual methods, which require the operator to position regions of interest (ROIs). In this study, three MTF determination methods were compared for RQA 3 and RQA 5 beam quality — two semi-automatic (ImageJ via the COQ plugin and IAEA ATIA) and one manual (the Coltman method) — using a Konica Altus DR digital radiology system in a large-scale hospital. The semi-automatic methods showed strong agreement with each other, with variations between 0.42 and 1.00 MTF units (%), while the manual method showed greater divergence from the other two, varying between 2.73 and 13.30 MTF units (%). It is concluded that semi-automatic methods are advantageous in terms of reproducibility and efficiency when compared to the manual method. It is the medical physicist's responsibility to weigh the applicability of each methodology within the reality of their institution.

Keywords: Digital Radiology; Spatial Resolution; Quality Control; MTF.

1. Introduction

A fundamental metric for assessing image quality in both conventional and digital X-ray equipment is Spatial Resolution. It is defined as the ability to distinguish two neighboring structures as separated (1). Although its execution is mandated by national regulations (2,3), there is no guidance on how to perform the test or on the technical parameters (such as peak voltage, current-time product, focus-to-detector distance, or the use of additional beam-hardening filters). It is up to the test performer to decide on these conditions.

Commonly, the spatial resolution test is performed qualitatively: there is a direct translation between the obtained radiographic image and the test result (in line pairs per millimeter). Figure 1 shows a test device that allows visual assessment of the results.

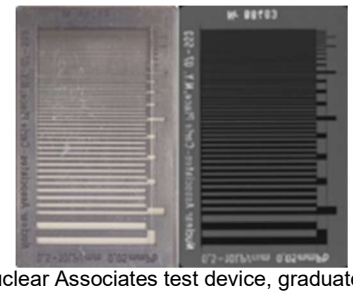

Figure 1. Nuclear Associates test device, graduated from 0.5 to 10.0 line pairs per millimeter (lp/mm). On the left, a photograph of the device; on the right, a radiographic image of the test device.

Although sufficient for regulatory compliance, visual assessment of the limiting spatial resolution does not fully characterize the system's ability to accurately reproduce structures as spatial frequency increases. Moreover, this approach introduces a degree of subjectivity into the evaluation. For a more robust and objective assessment, determination of the Modulation Transfer Function (MTF) is appropriate.

The MTF provides a comprehensive description of the system's ability to reproduce image details as a function of spatial frequency, relating system performance to the spatial frequency of the irradiated objects. It represents the ability to transmit input signal modulation at varying spatial frequencies (4).

The literature describes different methodologies for determining the MTF. In 2014, a plug-in for the ImageJ software was developed (5). This tool computes MTF from the profile of the edge spread function (ESF) of a slightly angled copper plate. In 2021, the International Atomic Energy Agency (IAEA) published Human Health Series No. 39 (6), describing a low-cost test device that also derives MTF from the ESF of a lightly tilted copper insert and provides dedicated software (ATIA) for this purpose. Figure 2 and Figure 3 depict the graphical interfaces of the software tools used in this study.

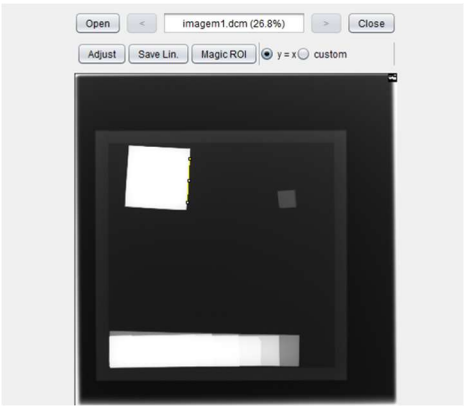

Figure 2. COQ software interface during MTF assessment.

More recently, in July 2024, the American Association of Physicists in Medicine (AAPM) released Report TG-150 (7), which presents guidelines for acceptance testing and quality control of digital radiography systems. The report proposes a

methodology based on direct evaluation of pixel intensities in a line-pair phantom. This approach was originally described by Coltman in 1954 and later adapted by Droege in 1982 for the evaluation of computed tomography systems (8,9).

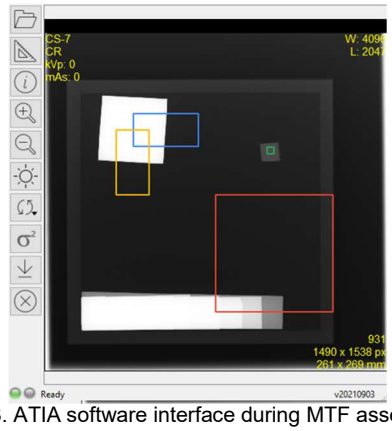

Figure 3. ATIA software interface during MTF assessment.

In this context, the present study aims to compare the performance, consistency, and practical applicability of two semi-automated MTF assessment methodologies (using ImageJ COQ plugin and the ATIA software from IAEA) with Coltman manual approach, as proposed by the AAPM, in a digital radiography system.

2. Materials and Methods

2.1. Phantoms

Two test phantoms were used in this study. The first was the Nuclear Associates 07-553 line-pair resolution plate (Figure 1), employed for MTF measurements using the Coltman method. The second phantom was the device recommended by the IAEA, consisting of a 28 cm × 28 cm × 0.5 cm PMMA plate containing a 5 cm × 5 cm × 0.2 cm copper square and a 1 cm × 1 cm × 0.4 cm aluminum insert, both mounted flush with the surface (Figure 2 and Figure 3). The copper square should be positioned with a slight tilt relative to the plate's edge to enable MTF measurement. Figures 2 and 3 illustrate radiographic images of this phantom.

2.2. Software Tools

Three software tools were used for analysis: (i) the COQ plugin for ImageJ, used to determine MTF using the IAEA phantom;

(ii) the ATIA software, implemented according to the methodology described in IAEA Human Health Series No. 39; and

(iii) MicroDicom (10), used to extract ROI measurements required for the manual Coltman-based method described by the AAPM.

2.3. Beam Characterization

All radiographs were acquired using a Konica Altus DR digital X-ray system at a large hospital. Post-processing was disabled for all images to ensure consistency across acquisitions. The beam quality used was RQA 3 and RQA 5, following IEC 62220-1 recommendations.

For each beam quality, both vertical and horizontal MTFs were measured, and evaluations were performed using the small focal spot.

2.4 Acquisition parameters

Table 1 provides a description of the key acquisition parameters used. The test devices were positioned centrally on the detector surface, aligned with the central X-ray beam. Care was taken to ensure that the phantom was placed flat, without tilt or rotation, and that its edges were parallel to the detector borders.

Table 1. Acquisition parameters used for image acquisition under RQA3 and RQA5 beam qualities.

	Values	
Parameter	RQA 3	RQA 5
kVp	50	70
Filtration (mm Al)	10	21
mAs	20	
SID (mm)	1000	
Field size (mm)	220 x 220	
Inherent filtration (mm Al)	2.7	
Grid use	No	
Detector mode	No binning	
Matrix size (pixels)	1744 x 2066	
Pixel size (µm)	200	

Source: The author (2026).

2.5. Determination of the MTFs

2.5.1. Using the COQ Plugin

The images used for MTF evaluation were acquired using a digital radiography system, with exposures performed on the phantom plate described in the IAEA report. These images were then processed using ImageJ with the COQ plugin, in which the copper edge region of the resolution phantom was selected.

Based on this edge delineation, the software generated the image MTF. The resulting MTF was subsequently compared with the measurements obtained using the other evaluation methods.

2.5.2. Using the ATIA Software

The images used for MTF evaluation were acquired using a digital radiography system, with exposures performed on the phantom plate described in the IAEA report. These images were then processed using the ATIA software, in which the MTF was

generated through analysis of the aluminum edge present in the phantom.

The MTF results obtained with this approach were subsequently compared with those derived from the other evaluated methods. The entire procedure was carried out semi-automatically, in accordance with the methodology described in the IAEA report.

2.5.3. Using the Coltman Method

Manual MTF measurements were performed using the Coltman method as described in the AAPM report. The cutoff frequency was defined according to Equation 1:

$$F_{max} = \frac{F_c}{3}, \quad (1)$$

where F_c is the maximum theoretical resolution of 5 line pairs per millimeter (lp/mm). Thus, the valid frequencies lie within the interval [0.93, F_{max}] lp/mm, where F_{max} is the highest visually distinguishable spatial frequency. The upper limit represents the mathematical reliability threshold for the Coltman transformation. Since the method converts Square Wave Response (CTF) to Sine Wave Response (MTF) via a Fourier series expansion, determining the MTF requires knowledge of the contrast at odd harmonics, specifically at 3f. Therefore, to ensure that the third harmonic does not exceed the system's maximum measurable frequency (F_c), the analysis is restricted to the interval where $f \leq \frac{F_c}{3}$.

Consequently, regions of interest (ROIs) were delineated around the sets of distinguishable spatial resolution groups in the radiographs. These groups corresponded to 1.2, 1.4, 1.7, 2.0, and 2.4 line pairs per millimeter. The MTF was computed for each spatial frequency using Equation 2:

$$MTF(ROI(i)) = \frac{222 * SD_{ROI(i)}}{AVG_{ROI1} - AVG_{ROI2}}, \quad (2)$$

where: AVG_{ROI} denotes the mean pixel value within the dark region of the radiograph at the lowest spatial frequency; AVG_{ROI2} denotes the mean pixel value within the bright region of the radiograph at the lowest spatial frequency; 222 is a dimensionless factor; and SD'(ROI_i) is given by Equation 3:

$$SD`(ROIi) = SD(ROI(i)) - \sqrt{\frac{1}{2} * SD`\left({ROI_{BG1}}^2 + {ROI_{BG2}}^2\right)}, \quad (3)$$

where: SD_{BG1}represents the standard deviation measured in a background region of the plate without test structures, and SD_{BG2} represents the standard deviation measured in the region containing the spatial frequencies of interest.

The additional term within the square root is a correction factor employed in previous studies for noise compensation (9). Figure 4 illustrates the placement of the ROIs on the radiograph of the test device. The ROIs were delineated by two independent observers following a standardized instruction: to position the ROIs over the set of line-pair groups that were visually resolvable according to the Coltman method description in the AAPM TG-150. Consensus was reached regarding both positioning and boundaries, thereby minimizing variability and reducing uncertainty in the analysis. Only spatial frequencies for which both observers reached agreement regarding the optimal ROI placement were considered in the analysis, ensuring consistency and reducing observer-dependent variability.

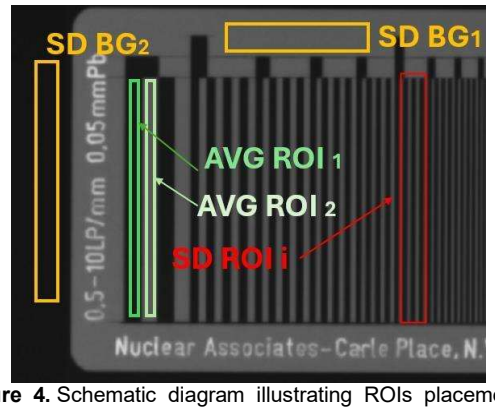

Figure 4. Schematic diagram illustrating ROIs placement for measuring the mean pixel value (MPV) and standard deviation (SD).

For each spatial frequency, four measurements of the mean pixel value (MPV) and standard deviation (SD) were acquired. The standard deviation was subsequently calculated for each frequency.

2.5. Method Comparison

The methods were compared based on the measured MTF values to assess their agreement across all configurations tested under RQA 5, in both vertical and horizontal orientations, for the small focal spot. A statistical analysis was performed on the MTF values measured by the COQ and ATIA methods to assess agreement, assuming a level of significance of 0.05.

3. Results

Figure 5 shows the measured MTF values for the small focal spot in both vertical and horizontal orientations for beam quality RQA 3.

Figure 6 shows the measured MTF values for the small focal spot in both vertical and horizontal orientations for beam quality RQA 5.

Across all four graphs, a consistent pattern is observed, with overlapping curves for the semi-automatic methods and a similar overall trend for the Coltman method, albeit with greater variability.

The largest absolute difference in MTF units (%) was calculated by the direct subtraction of the values obtained by the compared methods at the same spatial frequency using equation 4:

$$\Delta MTF(f) = 100 * |MTF_{method\ A}(f) - MTF_{method\ B}(f) \quad (4)$$

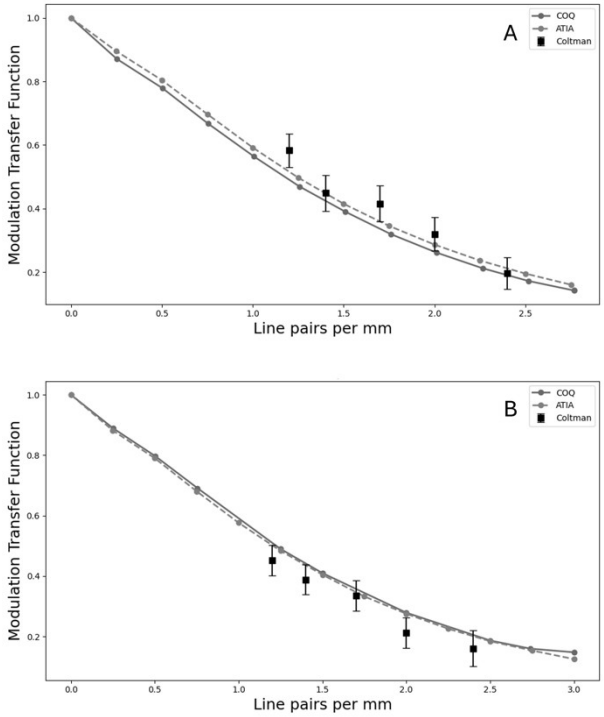

Figure 5. MTF assessed in (a) the vertical and (b) the horizontal directions for the RQA 3 beam quality.

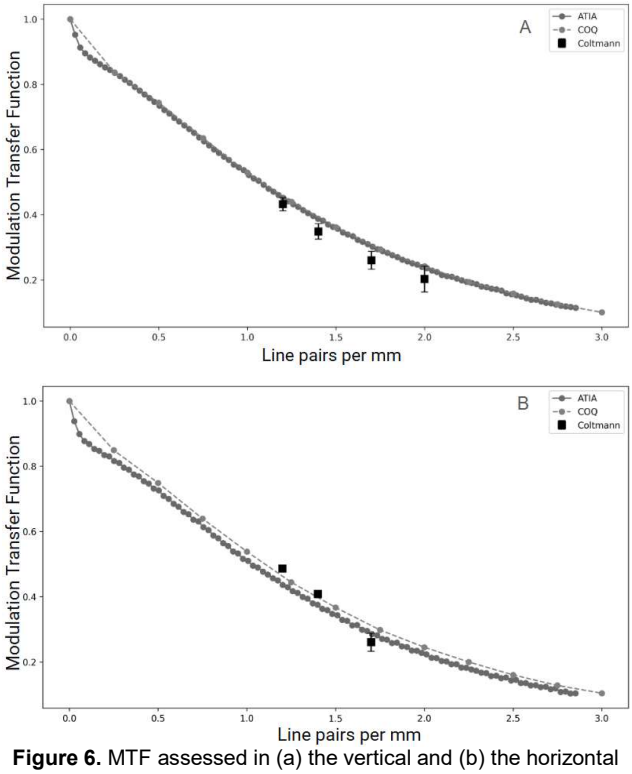

Figure 6. MTF assessed in (a) the vertical and (b) the horizontal directions for the RQA 5 beam quality.

Table 2 summarizes the maximum absolute differences for each pair of methods.

A Student's t-test was applied to the MTF values obtained by the semi-automatic methods. No statistically significant difference was found.

Table 2. Maximum absolute differences between methods for both axes and beam qualities.

	Horizontal Axis		Vertical Axis	
	RQA 3	RQA 5	RQA 3	RQA 5
COQ vs ATIA	1.00	1.00	0.85	0.42
COQ vs Coltman	11.05	3.35	12.40	2.73
ATIA vs Coltman	12.00	3.33	13.30	3.68

Source: The author (2026).

4. Discussion

Statistical testing indicated normality among the MTF values obtained using the COQ and ATIA semi-automated methods. The test device employed for these methods is inexpensive and easy to construct, eliminating the need for commercial line-pair phantoms. However, the main limitation is the absence of any qualitative assessment of image resolution. Nonetheless, the quantitative analysis provided by these methods enables rigorous technical monitoring of the system and the optimization of clinical protocols.

Overall, the results in Figures 5 and 6 show good agreement among the three methods. It is evidenced by the overlapping MTF curves obtained with the semi-automatic approaches for both beam qualities. The Coltman method also followed the same general trend, although with slight deviations. These findings indicate that all three methods provide coherent estimates of spatial resolution for the evaluated beam qualities. Therefore, the choice of method should be guided by practical considerations, such as ease of use, execution time, and reproducibility.

The Coltman method is inherently limited to nominal spatial frequencies defined by the line-pair phantom. This discretization prevents a continuous characterization of the MTF, particularly at very low frequencies, which are not adequately sampled by the phantom design. At the high-frequency end, the evaluation is further constrained by the detector pixel size, which imposes the Nyquist limit, as well as by practical difficulties in accurately positioning ROIs over fine line-pair patterns. As a result, the method does not allow a reliable determination of the system's limiting spatial resolution.

Furthermore, because it is a manual procedure, the Coltman method is time-consuming and depends heavily on precise ROI placement by the operator, which increases the uncertainty of the measurements. This effect is reflected by the higher standard deviations observed at higher spatial frequencies. Even slight angular misalignment of the line-pair plate can further compromise the accuracy of the MTF estimation.

This work demonstrates consistent agreement between methods across the evaluated acquisition conditions. Future investigations may extend this analysis to additional beam qualities, different detector technologies, other imaging modalities, and alternative phantoms to further assess method concordance. It is also important to compare these approaches with other MTF evaluation methodologies, particularly those based on computational techniques that rely on dedicated phantoms (11).

While the authors acknowledge the value of the AAPM-recommended method—particularly as an accessible alternative when more sophisticated computational tools are not available, and as a useful didactic resource for understanding the relationship between SD, MPV, and MTF—the manual approach remains less advantageous in terms of speed, reliability, and reproducibility when compared to the semi-automated methods.

5. Conclusions

This study demonstrates that while semi-automated tools like the ImageJ COQ plugin and ATIA software provide consistent results, the manual AAPM approach remains sensitive o operator-dependent factors. By minimizing human bias, semi-automated methods offer a more standardized and reproducible evaluation of the MTF. Ultimately, the choice of methodology rests with the medical physicist, who must balance the need for automated consistency against the specific clinical requirements and technical resources of their institution.

Ackowledgements

The authors gratefully acknowledge the support of the Laboratory of Applied Physics to Diagnostic Radiology (LAFAR), the Medical Physics and Radiation Protection Unit of the Clinical Hospital of the Botucatu Medical School (NFMRp/HCFMB), and the Institutional Scientific Initiation Scholarship Program, whose contributions were essential to the development of this work.

References

1. Benjamin MM, Shaker M, Rabbat MG. Assessing coronary artery disease using coronary computed tomography angiography. In: Cardiovascular and Coronary Artery Imaging. Elsevier; 2022. p. 129–45. doi:10.1016/B978-0-12-822706-0.00011-1
2. Ministério da Saúde - MS, Agência Nacional de Vigilância Sanitária - ANVISA. INSTRUÇÃO NORMATIVA - IN N° 90, DE 27 DE MAIO DE 2021. Dispõe sobre requisitos sanitários para a garantia da qualidade e da segurança em sistemas de radiografia médica convencional, e dá outras providências. 2021. p. 6–10.
3. Ministério da Saúde - MS, Agência Nacional de Vigilância Sanitária - ANVISA, Diretoria Colegiada. RESOLUÇÃO RDC Nº 611, DE 9 DE Março DE 2022. 2022 Mar 16.
4. Li Z, Zhou F, Yao H, Ci Z, Yang Z, Jin Z. Halide perovskites for high-performance X-ray detector. Materials Today. 2021 Sep; 48:155–75. doi:10.1016/j.mattod.2021.01.028
5. Schneider CA, Rasband WS, Eliceiri KW. NIH Image to ImageJ: 25 years of image analysis. Nat Methods. 2012 Jul 28;9(7):671–5. doi:10.1038/nmeth.2089
6. International Atomic Energy Agency - IAEA. IAEA HUMAN HEALTH SERIES NO. 39 - Implementation of a Remote and Automated Quality Control Programme for Radiography and Mammography Equipment. 2021.
7. American Association of Physics in Medicine. Acceptance Testing and Quality Control of Digital Radiographic Imaging Systems. 2024 jul.
8. Coltman JW. The specification of imaging properties by response-to a sine wave input. 1954.
9. Ronald T. Droege, Richard L. Morin. A practical method to measure the MTF of CT scanners. Med Phys. 1982;9(5).
10. MicroDicom - free DICOM viewer for Windows [Internet]. [cited 2025 Feb 23]. Available from: https://www.microdicom.com/
11. Francisco MFF, Souza DLM, Medeiros RB, De Freitas MB, Pires SR. Método de avaliação da resolução espacial em sistemas digitais de mamografia através do uso da MTF. Revista Brasileira de Física Médica. 2019 Feb 3;12(3):26. doi:10.29384/rbfm. 2018.v12.n3.p26-29

Contact:

Diana Rodrigues de Pina
Department of Infectious Diseases, Dermatology, Diagnostic Imaging and Radiotherapy, Botucatu School of Medicine, São Paulo State University (UNESP)
Botucatu, 18618-000, São Paulo, Brazil
E-mail: diana.pina@unesp.br